Appl. Phys. A 69 [Suppl.], S935–S939 (1999) / Digital Object Identifier (DOI) 10.1007/s003399900271

Applied Physics A
Materials
Science & Processing

193-nm laser ablation of CVD diamond and graphite in vacuum: plume analysis and film properties

R.J. Lade, F. Claeyssens, K.N. Rosser, M.N.R. Ashfold*

School of Chemistry, University of Bristol, Bristol BS8 1TS, UK

Received: 21 July 1999/Accepted: 11 September 1999/Published online: 28 December 1999

Abstract. The pulsed laser ablation of chemical vapor deposition (CVD) diamond and graphite samples in vacuum has been investigated by the use of an ArF excimer laser operating at $\lambda = 193$ nm. The composition and propagation of both ablation plumes has been probed via wavelength and spatially and temporally resolved measurements of the plume emission and found to be very similar. Electronically excited C atoms and C^+ and C^{2+} ions are identified among the ablated material. Plume expansion velocities are estimated from time-gated imaging of specific C and C^+ emissions. Langmuir probe measurements provide further insight into the propagation of the charged components in both ablation plumes. Diamond-like carbon (DLC) films grown by 193-nm laser ablation of both target materials on Si substrates maintained at room temperature have been investigated by laser Raman spectroscopy (325 nm and 488 nm excitation) and by both optical and scanning electron microscopy, and their field emission characteristics investigated. Again, similarities outweigh the differences, but DLC films grown from ablation of the diamond target appear to show steeper I/V dependencies once above the threshold voltage for field emission.

PACS: 81.15.Fg; 79.20.DS; 68.55.-a

Pulsed laser ablation (PLA) of a graphite target in vacuum is receiving increased attention as a room temperature route to producing thin hydrogen-free diamond-like carbon (DLC) films on a variety of substrate materials [1]. Prior research has established that the plume accompanying PLA of graphite at long excitation wavelengths (e.g., 1064 nm) contains a high proportion of small carbon cluster species (ions and neutrals) [2, 3]; DLC films containing an estimated 70% sp^3 hybridized C atoms have been reported following 1064-nm laser ablation of graphite, in vacuum, but only at laser intensities approaching 10^{10} W cm^{-2} [4]. Conversely, the plume arising when PLA is induced by 193-nm radiation is dominated by atomic species (C neutrals and ions) [5], and high-quality DLC films containing $> 90\%$ sp^3 bonded C have been produced with intensities as low as $I \sim 5 \times 10^8$ W cm^{-2} [4–8]. Such observations support the consensus view that high-impact (~ 100 eV) energies are required for formation of sp^3 (rather than graphitic) networks in the deposited film, and that high ejection velocities are a feature of electronic (i.e., ultraviolet) rather than thermally driven material ablation. Nonetheless, many details of the ablation process, and of the way in which the plume composition and properties influence the various film characteristics, still merit further study. One aspect of particular interest is the origin and suppression of isolated 'macroparticles' in such DLC films [9–11]. In the case of dense graphite targets, macroparticles are envisaged to arise as a result of rapid, localized (laser-induced, in the case of PLA) heating of small gas pockets trapped in pores lying close below the surface and within the focal volume. The subsequent gas expansion results in ballistic ejection of surface material, including macroparticles [12].

Polycrystalline diamond, grown by chemical vapor deposition (CVD) methods, has higher density and lower porosity than even the most dense graphite samples, and was thus considered as a possible alternative target material suitable for DLC film growth by ultraviolet (UV) pulsed laser ablation. This paper reports PLA of both graphite and thick ($> 100\,\mu$m) polycrystalline diamond targets brought about by ArF ($\lambda = 193$ nm) laser pulses, in vacuum. Wavelength, spatially and temporally resolved measurements of the emission from electronically excited species arising in these two PLA processes yield very comparable results, as do Langmuir probe time-of-flight (TOF) measurements of the positively charged particles in both plumes. These findings, and companion analyses of the deposited DLC films by laser Raman spectroscopy and scanning electron microscopy (SEM), suggest that PLA of CVD diamond at 193 nm is preceded by local surface graphitization; minor differences in the field emission characteristics of DLC films deposited using the different target materials appear to correlate with reduced sur-

*Corresponding author.
(Fax: +44-117/925-1295, E-mail: mike.ashfold@bris.ac.uk)

COLA'99 – 5th International Conference on Laser Ablation, July 19–23, 1999 in Göttingen, Germany

face damage and an enhanced macroparticle density in the films derived from CVD diamond.

1 Experiment

Much of the apparatus, which is shown schematically in plan view in Fig. 1, and the experimental procedure has been reported previously [5], and is only summarized here. The output of an excimer laser (Lambda-Physik, Compex 201) operating on ArF (193 nm, 10 Hz repetition rate, output energy $\leq 300\,\mathrm{mJ\,pulse^{-1}}$) is steered using two (or three) dichroic mirrors and focused (20-cm f.l. lens) so as to be incident on a target mounted on a microprocessor controlled 2-D translation stage (PIC based Stamp2) located in a stainless steel vacuum chamber maintained at $\sim 10^{-6}$ Torr. As Fig. 1 illustrates, this chamber is also equipped with (i) a quadrupole mass spectrometer (Hiden, EQP HAS-SPL-4353) and (ii) a user-rotatable carousel capable of supporting up to six $1\,\mathrm{cm^2}$ substrates, the axes of both of which are mounted in the horizontal plane at $\sim 45°$ on either side of the incident laser beam; (iii) a 100-mm turbomolecular pump backed by a rotary pump, appropriate pressure gauges, venting ports, power and signal feed-throughs (e.g., for Langmuir probe measurements), facility for introducing metered gas flows and, in the top flange, a large quartz viewing port. The front face of the target is on the center axis of the chamber. The target mount may be rotated about this vertical axis manually, and locked at any user-selected orientation relative to the laser beam. For the film deposition reported here, the target was oriented at 45° to the incident laser beam, with its surface normal directed towards the substrate. The programmable mount allows the target to be rastered relative to the fixed laser focus, thereby allowing each laser shot to ablate a fresh area of the target. Target materials investigated in this work were high-density graphite (Poco Graphite Inc., DFP-3-2 grade) and CVD diamond. The latter was grown in-house (at growth rates $\sim 100\,\mu\mathrm{m\,hr^{-1}}$) by the use of a DC plasma jet system operating with a $CH_4/H_2/Ar$ gas mixture at a pressure ~ 50 Torr. The focal spot on the target had an area $\sim 0.4\,\mathrm{mm} \times 1\,\mathrm{mm}$, reflecting the rectangular spatial profile of the laser output. The long axis of this profile is normally aligned vertically in the labaratory frame, but can be rotated through 90° by introduction of the third steering mirror.

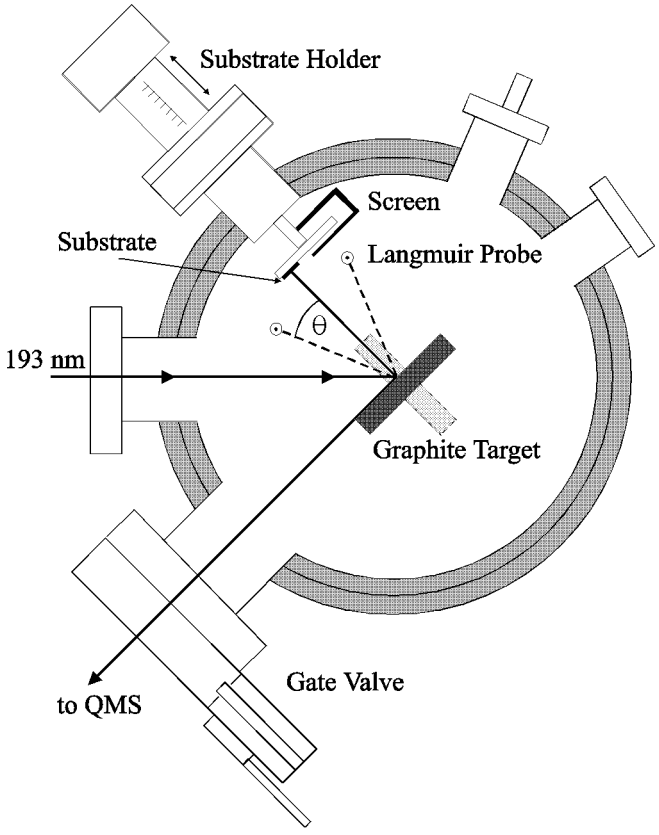

Fig. 1. Plan view of the ablation chamber. QMS=quadrupole mass spectrometer. The graphite target is shown oriented for film deposition (*dark*) and is rotated through 90° (*dashed*) for QMS analysis. The angle θ is defined relative to the surface normal, with positive θ towards the laser propagation axis

The ablation plume and the focal volume adjacent to the target are both clearly visible via their accompanying optical emission. This can be viewed by use of a quartz fiber bundle located behind a lens/iris combination and the observation port in the top flange. This arrangement restricts the viewing zone to a column about 2 mm in diameter. The other end of the fiber bundle abuts the front slit of a 12.5-cm monochromator (Oriel Instaspec IV, 600 lines/mm ruled grating) equipped with a UV extended CCD array detector. Emission from selected excited species was also investigated by the substitution of a CCD camera (Photonic Science) equipped with a time-gated ($\Delta t = 100$ ns) image intensifier in place of the lens/fiber bundle assembly and viewing through an appropriate narrow band interference or short-pass cutoff filter; such images afford a particularly clear visualization of the temporal and spatial evolution of selected species within the ablation plume [4, 5, 13, 14]. Complementary measurements of the TOF (and thus velocity) distributions of positively (and negatively) charged particles in the ablation plume were obtained by the use of up to four suitably biased W wires (125 μm in diameter) as simple electrostatic Langmuir probes, and the monitoring of the post-ablation current pulse via a fast oscilloscope (LeCroy 9361) and PC.

Films were deposited on precleaned Si(100) and quartz substrates, under vacuum, at a variety of laser fluences and for a range of deposition periods (≤ 15 min). They were subsequently analyzed by optical and scanning electron microscopy (SEM), laser Raman spectroscopy (LRS) at two different excitation wavelengths (325 and 488 nm), and their field emission characteristics tested using a purposely designed test station, the design and operation of which have been described in detail elsewhere [15, 16].

2 Results and discussion

2.1 Plume Diagnostics

At any given fluence, the optical emissions accompanying 193-nm PLA of graphite and CVD diamond in vacuum appear very similar both to the naked eye and even when subjected to detailed spectroscopic analysis. At low pulse energies, the plume appears as a small volume of intense

white plasma at the laser focus, together with a more extensive diffuse green glow, distributed symmetrically about the surface normal and filling most of the forward hemisphere. Superimposed on this are occasional thin bright tracks originating from the focal region; these we associate with incandescent sputtered macroparticles. At higher fluences, the emission from both target materials is supplemented by a narrow shaft of purple emission, which also appears to emanate from the focal spot and maximize in the solid angle between the laser propagation axis and the surface normal. This is illustrated by Fig. 2, which compares wavelength dispersed ($350 \leq \lambda \leq 1000$ nm) plume emission spectra measured during PLA of CVD diamond (a,c) and graphite samples (b,d), by the use of 200-mJ, vertically oriented, 193-nm laser pulses incident at 45° to the surface normal, and monitored 3 mm from the target along axes defined by $\theta = +22°$ (i.e., in the purple shaft) (a,b) and again at 3 mm along $\theta = -22°$ (c,d). These spectra were produced by the combination of overlapping 300-nm sections recorded by the use of the Instaspec IV system (3-sec accumulations). They have not been corrected for the wavelength dependence of the quartz fiber bundle transmission, the grating reflectivity, or the efficiency of the CCD array detector; the overall detection sensitivity peaks at about 620 nm and is reduced by a factor of about 3 at the extremes of the displayed range. As was noted previously [5], the spectra are made up entirely of emissions from C, C^+, and C^{2+} species [17, 18], with relative intensities that are both fluence and spatially dependent. C^{2+} emissions (which appear as second-order features in the wavelength range displayed) are only observed within a few mm of the target. C^+ ions are identified as the carrier of the localized shaft of purple emission; no C^+ emissions are evident in the spectra recorded along the $\theta = -22°$ axis. The observed directionality of this shaft, which we find to depend sensitively on the orientation of the rectangular laser pulse, reinforces previous suggestions that the observed ionic emissions arise from laser–plume rather than laser–target interactions [5]. Both the C^{2+} and C^+ emission intensities fade (relative to that from neutral C atoms) as the viewing zone is moved further from the target.

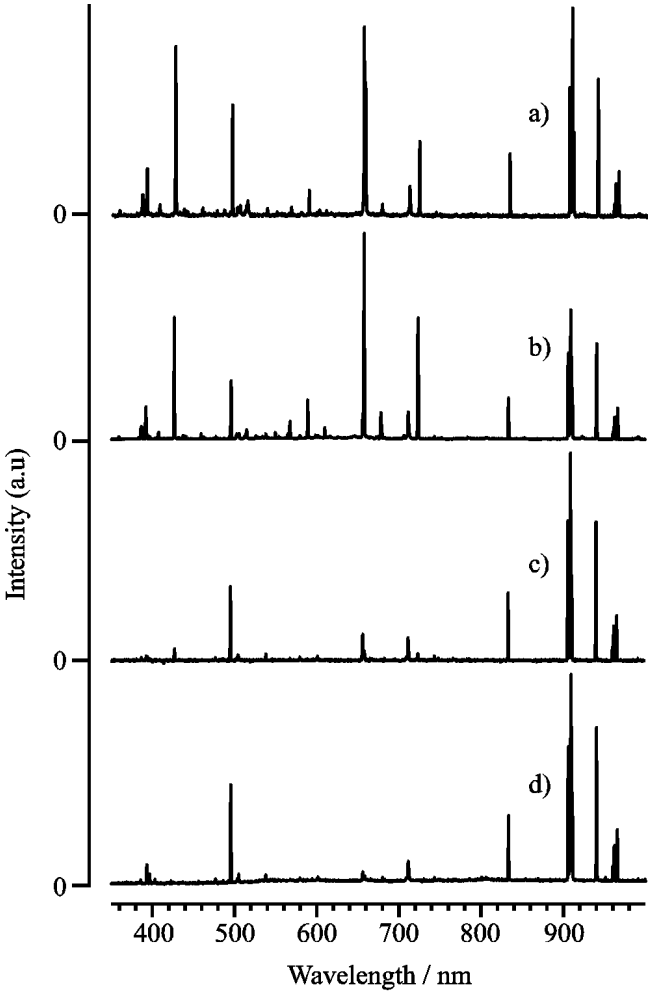

Fig. 2a–d. Wavelength dispersed spectra of the plume emission accompanying PLA of CVD diamond (**a**,**c**) and graphite samples in the range 350−1000 nm (**b**,**d**), obtained using 200-mJ, vertically oriented, 193-nm laser pulses. The emission was monitored 3 mm from the target along $\theta = +22°$ (**a**,**b**) and $\theta = -22°$ (**c**,**d**)

Time-gated CCD images of the 426.7-nm C^+ $4f^{1;2}F^0 \rightarrow 3d^{1;2}D$ doublet emission arising in the 193-nm PLA of CVD diamond yield estimates of the propagation velocity of the center of gravity of this C^+ emission feature ($v_+ \sim 3.2 \times 10^4$ m s^{-1}) that are virtually identical to those obtained in our earlier studies involving graphite targets. As in the earlier work [5], electrostatic probe studies remind us that the C^+ ions revealed via the purple shaft are only a minor fraction of the total ion flux in the ablation plume, and that positively charged material (in nonemitting states) is distributed throughout the forward hemisphere. These measurements, which reveal comparable ion fluxes at $\theta = +22°$ and $-22°$ (although the former consistently displays a mean propagation velocity of $\bar{v}_+ \sim 4.5 \times 10^4$ m s^{-1}, which is $\sim 20\%$ higher than that observed at $\theta = -22°$), provide further support for the presumed similarity of the plumes arising in the 193-nm PLA of graphite and CVD diamond.

2.2 Film diagnostics

Obtaining sufficiently sharp SEM cross section images of the DLC films produced in this work to allow reliable estimation of the film thickness proved difficult. However, guided by our previous studies of the 193-nm PLA of graphite in vacuum [11] (which suggested deposition rates of ~ 7 pm pulse^{-1}), we estimate that the typical film deposited here by the use of 200-mJ pulses with 10-Hz repetition rate and 15 min duration had a thickness of ~ 50 nm. Optical microscopy reveals some raised vein-like structures in the films deposited from both target materials when longer durations or higher pulse energies are used. We take this as an indication of the early stages of film delamination, reflecting the buildup of compressive stresses. Given the very similar plume compositions from 193-nm PLA of CVD diamond and graphite (above), and the observation that such structures appear in films deposited under equivalent conditions from both target materials, we surmise that both yield similar deposition rates.

Figure 3 shows six laser Raman spectra (LRS). Figures 3a and 3b show the as-grown CVD diamond and the high-density graphite targets, respectively; Fig. 3c shows the CVD diamond film surface post-ablation; and Figs. 3d and 3e show spectra of the DLC films grown by PLA of these respective

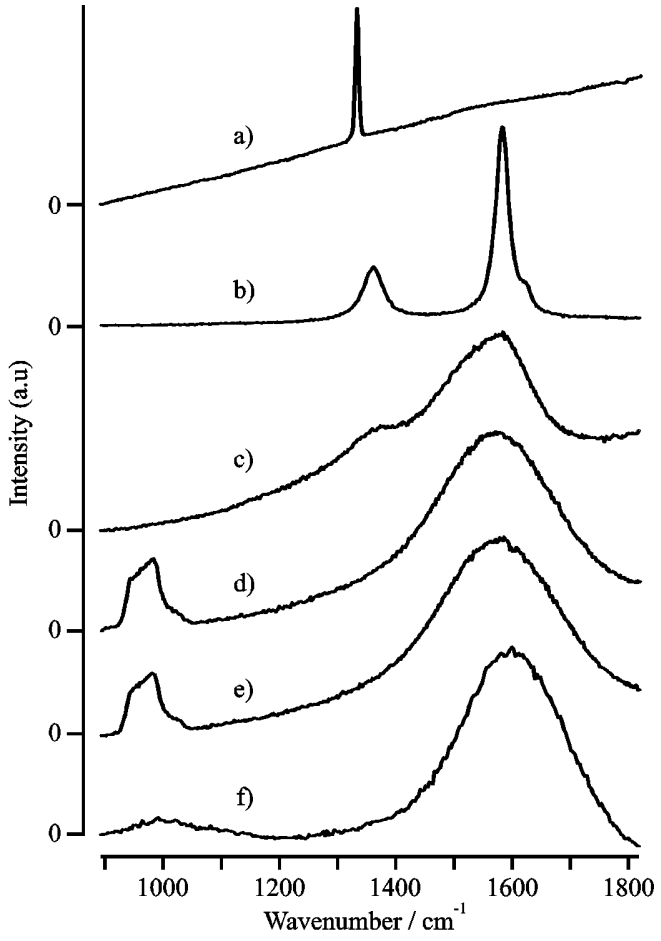

Fig. 3. Laser Raman spectra of the: as-grown CVD diamond target (a); high-density graphite target (b); CVD diamond film surface post-ablation (c); DLC film grown by 193-nm PLA of CVD diamond (d); and DLC film grown by 193-nm PLA of graphite (e). Each were recorded with an excitation wavelength of 488 nm. In (f) is shown a Raman spectrum of the same film as in (e) but recorded using 325-nm excitation

targets. These five spectra were all recorded using 488-nm Ar^+ laser excitation. Figure 3f displays a Raman spectrum of the same film as in Fig. 3e but recorded with 325-nm excitation. Clearly, LRS of the deposited DLC films (Fig. 3d,e) provides yet more support for the view that there is little difference in the ablated material resulting from 193-nm irradiation of graphite and CVD diamond. Some rationale for this finding comes from comparing the spectra in Figs. 3a, b, and c. The strong 1332 cm^{-1} peak in Fig. 3a highlights the high quality of the CVD diamond surface, yet post-ablation (Fig. 3c) LRS shows little evidence for diamond. All of the present observations are explicable if one assumes that the initial stages of the PLA of CVD diamond in vacuum at 193 nm involve very rapid, localized surface graphitization prior to material injection into the gas phase. Such an explanation suggests that it could be rewarding to perform similar PLA studies using much longer excitation wavelengths, for which the respective target absorption properties are less similar, or with much shorter (sub-ps) pulse durations, which in the case of CVD diamond might be insufficient to allow efficient graphitization.

The differences between the spectra in Figs. 3e and 3f merits comment. The strong feature centered in Fig. 3e at a Stokes shift of $\sim$ 965 cm^{-1} is a signature of the Si substrate. The relative showing of this peak decreases with decreasing excitation wavelength (see also [19]), reflecting the increasing absorption coefficient of the deposited DLC coating at shorter wavelengths and the consequent reduction in the penetration depth achieved by the Raman exciting laser. Closer inspection of these spectra, and of those taken previously for similar DLC films using 632.8-nm He-Ne laser excitation [11], reveals a noticeable and systematic shift in the peak of the broad asymmetric Raman profile traditionally associated with DLC, from $\sim$ 1485 cm^{-1} (632.8-nm excitation), through $\sim$ 1560 cm^{-1} (488 nm (e)) to $\sim$ 1595 cm^{-1} (325 nm (f)). This suggests that, as is widely recognized for the case of polycrystalline CVD diamond, the detailed form of the Raman spectrum obtained for any given DLC film will be sensitive to the excitation wavelength used.

Only in the electron emission properties was there any, albeit tentative, evidence for differences in the DLC films resulting from 193-nm PLA of CVD diamond and high-density graphite targets, each deposited by the use of 200-mJ pulses with a 10-Hz repetition rate for a 15-min. duration. Figure 4 shows measurements of emission current (I) as a function of bias voltage (V) for DLC films grown from both CVD diamond and graphite targets. Such $I - V$ curves were measured by the ramping of V up and down repeatedly (sweep rate $\sim$ 25 V s^{-1}); their reproducibility improved after the first few up–down cycles, but SEM analysis revealed that this 'conditioning' does affect the film morphology in the immediate vicinity of the emission sites. Measurements were made at three different anode–surface separations (20, 40, and 60 μm), at several sites on each film, and for at least two films deposited from each target material. The DLC films derived

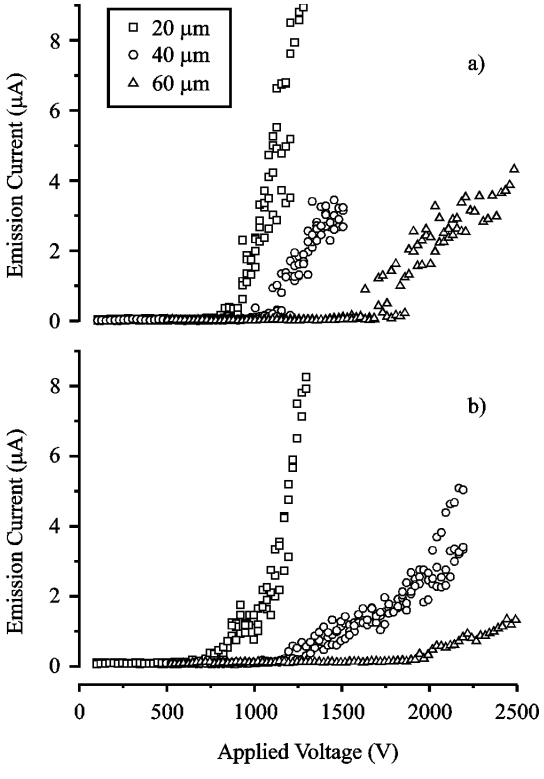

Fig. 4a,b. $I - V$ curves for DLC films grown on Si(100) by 193-nm PLA of CVD **a** diamond and **b** graphite obtained using 20- (□), 40- (○), and 60-μm (△) anode-surface separations

from these two sources show very similar threshold voltages, but once above the threshold, films grown from CVD diamond appear to show a steeper slope, implying larger $\mathrm{d}I/\mathrm{d}V$. Such behavior may correlate with the density of larger ($>$ 1-μm wide) macroparticles in the film, which both optical microscopy and SEM images suggest is considerably higher in the case of the film deposited from CVD diamond. Such a finding, which at first sight appears counterintuitive given the proposed mechanisms for macroparticle ejection and the higher density and lower porosity of diamond, might well be dependent on the CVD diamond growth rate. Diamond samples such as those used here, deposited at high growth rates by use of a plasma jet, are likely to contain more voids (and thus trapped gas pockets) than the smaller grain size films produced in most low-power CVD reactors. Future PLA studies, employing a range of CVD diamond targets with different grain sizes and morphologies, should allow us to check the validity of this proposal.

3 Conclusions

The 193-nm PLA of both CVD diamond and graphite samples, in vacuum, have been compared and contrasted, both from the perspective of the ablation plume and by investigation of the resulting DLC films deposited on Si(100). The composition and propagation of the plumes from both targets have been probed via wavelength and spatially and temporally resolved studies of the plume emission and by Langmuir probe TOF methods and found to be very similar. The deposited DLC films, grown on Si substrates maintained at room temperature, were studied by laser Raman spectroscopy, by both optical and scanning electron microscopy, and their field emission characteristics investigated. Again, similarities outweigh the differences, but DLC films grown from ablation of the diamond target appear to show steeper I/V dependencies once above the threshold voltage for field emission.

Acknowledgements. We are grateful to the EPSRC for financial support in the form of equipment grants, a Senior Research Fellowship (MNRA) and studentships (RJL and FC). We also thank Dr. P.W. May, M.-T. Kuo, J.A. Smith, P.A. Cook, G. Evans, and S. Charles (Dept. of Physics, University of Bristol) for their many and varied contributions to this work.

References

1. A.A. Voevodin, M.S. Donley: Surf. Coat. Technol. **82**, 199 (1996) and references therein
2. J.J. Gaumet, A. Wakisaka, Y. Shimizu, Y. Tamori: J. Chem. Soc., Faraday Trans. **89**, 1667 (1993)
3. S.M. Park, J.Y. Moon: J. Chem. Phys. **109**, 8124 (1998)
4. D.B. Geohegan, A. Puretzky: Mater. Res. Soc. Symp. Proc. **397**, 55 (1996) and references therein
5. R.J. Lade, M.N.R. Ashfold: Surf. Coat. Technol. (in press)
6. D.L. Pappas, K.L. Saenger, J.J. Cuomo, R.W. Dreyfus: J. Appl. Phys. **72**, 3966 (1992)
7. F. Xiong, Y.Y. Yang, V. Leppert, R.P.H. Chang: J. Mater. Res. **8**, 2265 (1993)
8. V.I. Merkulov, D.H. Lowndes, G.E. Jellison, Jr., A.A. Puretzky, D.B. Geohegan: Appl. Phys. Lett. **73**, 2591 (1998)
9. *Pulsed Laser Deposition of Thin Films*, ed. by D.B. Chrisey, G.K. Huber (Wiley, New York 1994)
10. F. Davanloo, J.H. You, C.B. Collins: J. Mater. Res. **10**, 2548 (1995)
11. S.E. Johnson, M.N.R. Ashfold, M.P. Knapper, R.J. Lade, K.N. Rosser, N.A. Fox, W.N. Wang: Diamont Relat. Mater. **6**, 569 (1997)
12. A. Anders: Surf. Coat. Technol. (1999, in press)
13. A.A. Puretzky, D.B. Geohegan, G.E. Jellison, Jr., M.M. McGibbon: Appl. Surf. Sci. **96**, 859 (1996)
14. A. Neogi, A. Mishra, R.K. Thareja: J. Appl. Phys. **83**, 2831 (1998)
15. P.W. May, S. Höhn, M.N.R. Ashfold, W.N. Wang, N.A. Fox, T.J. Davis, J.W. Steeds: Diamont Films Technol. **8**, 237 (1998)
16. M.-T. Kuo, P.W. May, A. Gunn, J.C. Marshall, M.N.R. Ashfold, K.N. Rosser: Int. J. Mod. Phys. B (in press)
17. W.L. Wiese, M.W. Smith, B.M. Miles: *Atomic Transition Probabilities*, Vol. 1 (NSRDS-NBS 4 1966)
18. A.R. Striganov, N.S. Sventitskii: *Tables of Spectral Lines of Neutral and Ionised Atoms* (IFI/Plenum, New York 1968)
19. T.A. Friedmann, J.P. Sullivan, J.A. Knapp, D.R. Tallant, D.M. Follstaedt, D.L. Medlin, P.B. Mirkarimi: Appl. Phys. Lett. **71**, 3820 (1997)